

The dynamics of the gradient of potential vorticity

This article has been downloaded from IOPscience. Please scroll down to see the full text article.

2010 J. Phys. A: Math. Theor. 43 172001

(<http://iopscience.iop.org/1751-8121/43/17/172001>)

[The Table of Contents](#) and [more related content](#) is available

Download details:

IP Address: 129.31.243.6

The article was downloaded on 13/04/2010 at 10:31

Please note that [terms and conditions apply](#).

FAST TRACK COMMUNICATION

The dynamics of the gradient of potential vorticity

J D Gibbon and D D Holm

Department of Mathematics, Imperial College London SW7 2AZ, UK

E-mail: j.d.gibbon@ic.ac.uk and d.holm@ic.ac.uk

Received 17 February 2010, in final form 17 March 2010

Published 13 April 2010

Online at stacks.iop.org/JPhysA/43/172001**Abstract**

The transport of the potential vorticity gradient ∇q along surfaces of constant potential temperature θ is investigated for the stratified Euler, Navier–Stokes and hydrostatic primitive equations of the oceans and atmosphere, in terms of the divergence-less flux vector $\mathcal{B} = \nabla Q(q) \times \nabla \theta$, for any smooth function Q of the potential vorticity q . The flux vector \mathcal{B} is shown to satisfy a transport equation reminiscent of that for magnetic field flux in magnetohydrodynamics. The result may apply to satellite observations of potential vorticity and potential temperature at the tropopause.

PACS numbers: 47.10.–g, 47.10.–A, 92.60.Aa, 92.60.Xg

1. Introduction

Potential vorticity (PV) is believed to be a particularly significant quantity in the dynamics of the atmosphere and the oceans [1, 2]. For an incompressible fluid the PV density is defined as $q = \omega \cdot \nabla \theta$, where $\omega = \text{curl } \mathbf{u}$ is the vorticity for a fluid with a divergence-less velocity field \mathbf{u} and θ is the potential temperature. This communication exposes a mechanism for creating the large gradients in potential vorticity density ∇q . Its discussion is based on the geometric properties of transport of intersections of level sets of the quantities q and θ encoded in the vector $\mathcal{B} = \nabla Q(q) \times \nabla \theta$ which turns out to obey an evolution equation of the form¹

$$\partial_t \mathcal{B} - \text{curl}(\mathcal{U} \times \mathcal{B}) = \mathcal{D}. \quad (1.1)$$

Here, the vector field \mathcal{U} is formally a transport velocity and will be derived explicitly below in several different cases. The quantity \mathcal{D} expresses the rate of change of the flux of \mathcal{B} in a frame moving with velocity \mathcal{U} . When $\mathcal{D} = 0$, the flux of \mathcal{B} is said to be *frozen* into the flow with velocity $\mathcal{U} = \mathbf{u}$. The Euler equations for the stretching and folding of vorticity, and the ideal MHD equations for the frozen-in transport of the flux of divergence-free magnetic field, both take the form (1.1) with $\mathcal{D} = 0$ (see [3–5]). However, the vector \mathcal{B} turns out to be

¹ The vector $\mathcal{B} = \nabla Q(q) \times \nabla \theta$ has been discussed in [3–5] and should not be confused with the cross product $\nabla B \times \nabla \theta$ considered in [6], in which the scalar B is a steady Bernoulli function.

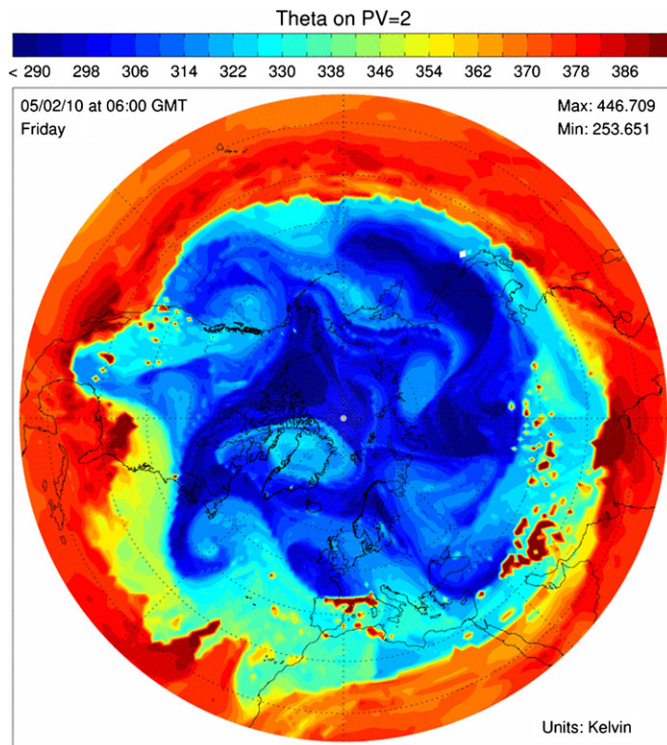


Figure 1. A typical snapshot of satellite data taken every 6 h of the Northern Hemisphere from ECMWF [7] shows contours of potential temperature θ on a level set of potential vorticity $q = 2$ located near the tropopause. Note that high gradients of θ lie at the sharp interfaces of the contours. (This figure is in colour only in the electronic version)

a wise choice even with dissipation: the vorticity dynamics of the Navier–Stokes equations with viscosity and the magnetic field evolution in MHD with resistivity, both take the form of equation (1.1) but, because $\mathcal{D} \neq 0$, the corresponding fields are no longer frozen into the flow. Figure 1 shows (model assimilated) satellite data for contours of potential temperature θ on the constant level surface of potential vorticity $q = 2$, which lies near the tropopause. See [7] for animations of this data in frames taken every 6 h. In these animations, the evolution of the contours of θ on a level set of potential vorticity $q = 2$ is seen: its appearance suggests the *stirring* of one liquid in another by stretching and folding, such as cream in black coffee.

The object of the present work is to derive exact equations of the form (1.1) for the evolution of the intersections of level sets of q and θ , in which we will find that \mathcal{D} is given by the divergence-less vector

$$\mathcal{D} = -\nabla[qQ'(q)\text{div}\mathcal{U}] \times \nabla\theta, \tag{1.2}$$

for any choice of the smooth function Q , and the vector \mathcal{U} will be derived in several cases.

Equations (1.1) and (1.2) are first derived in section 2 in the narrower setting of the Euler and Navier–Stokes equations. In section 3 the corresponding results are derived for the viscous hydrostatic primitive equations (HPE), which are commonly used in numerical simulations of the weather, climate and oceans. The stretching and folding mechanism inherent in (1.1) in

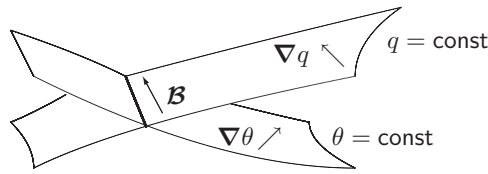


Figure 2. For the incompressible Euler equations in three dimensions, the vector $\mathcal{B} = \nabla Q(q) \times \nabla \theta$ is tangent to the curve defined by the intersection of the two surfaces $q = \text{const}$ and $\theta = \text{const}$.

the context of the viscous HPE may have some application to potentially rapid growth of ∇q in the atmosphere and oceans, where the occurrence of extreme events is of interest for the prediction of variability of the climate. In fact it has recently been shown by Cao and Titi [8] that the solutions of the viscous HPE remain regular (see also [9]). It follows that if extreme events do occur in solutions of HPE, then these must actually be smooth at sufficiently small scales. Conversely, HPE dynamics, although now known to be regular, may still produce extreme events due to the allowed intense stretching and folding of ∇q and $\nabla \theta$ under the dynamics of equations (1.1) and (1.2).

2. Summary of main results for the Euler and Navier–Stokes equations

Consider the dimensionless form of the incompressible 3D Euler and Navier–Stokes equations

$$\frac{D\mathbf{u}}{Dt} + \theta \hat{\mathbf{k}} = Re^{-1} \Delta \mathbf{u} - \nabla p, \quad \frac{D}{Dt} = \partial_t + \mathbf{u} \cdot \nabla, \quad (2.1)$$

where the temperature $\theta(\mathbf{x}, t)$ evolves according to

$$\frac{D\theta}{Dt} = (\sigma Re)^{-1} \Delta \theta. \quad (2.2)$$

Information about $\nabla \theta$ is needed to determine how $\theta(\mathbf{x}, t)$ might accumulate into large local concentrations. The traditional approach is to study this question through the dynamics of the potential vorticity, defined by ($\boldsymbol{\omega} = \text{curl } \mathbf{u}$ is the vorticity)

$$q := \boldsymbol{\omega} \cdot \nabla \theta. \quad (2.3)$$

The main results for the incompressible Euler and Navier–Stokes equations are summarized in the following.

Theorem 1. *In the cases below, q and θ satisfy*

$$\partial_t q + \text{div}(q\mathbf{U}) = 0, \quad \partial_t \theta + \mathbf{U} \cdot \nabla \theta = 0, \quad (2.4)$$

and, with $Q(q)$ as any smooth function of q , the divergence-free flux vector

$$\mathcal{B} = \nabla Q(q) \times \nabla \theta, \quad (2.5)$$

satisfies the stretching relation

$$\partial_t \mathcal{B} - \text{curl}(\mathbf{U} \times \mathcal{B}) = \mathcal{D}. \quad (2.6)$$

The divergence-less vector \mathcal{D} in (2.6) is given by $\mathcal{D} = -\nabla(qQ' \text{div } \mathbf{U}) \times \nabla \theta$.

(1) *For the incompressible Euler equations, $\mathbf{U} = \mathbf{u}$ and thus $\mathcal{D} = 0$. In this case $Dq/Dt = 0$, so the intersections of the level sets of q and θ shown in figure 2 move together with the fluid velocity, \mathbf{u} ;*

(2) For the incompressible Navier–Stokes equations, \mathcal{U} is defined as

$$q(\mathcal{U} - \mathbf{u}) = -Re^{-1}\{\Delta\mathbf{u} \times \nabla\theta + \sigma^{-1}\boldsymbol{\omega}\Delta\theta\}, \quad q \neq 0. \quad (2.7)$$

Moreover, for any surface $S(\mathcal{U})$ moving with the flow \mathcal{U} , one finds

$$\frac{d}{dt} \int_{S(\mathcal{U})} \mathcal{B} \cdot d\mathbf{S} = \int_{S(\mathcal{U})} \mathcal{D} \cdot d\mathbf{S}. \quad (2.8)$$

Remark. The three-dimensional incompressible Navier–Stokes equations possess only Leray’s weak solutions, while the Euler equations do not even possess these. Thus, the manipulations used in deriving (2.4)–(2.8) should be considered as purely formal.

Sketch proof of (2.4)–(2.8). The derivation of (2.4) follows the same standard manipulations that appear in the elegant classic proof of Ertel’s theorem [10], namely

$$\begin{aligned} \frac{Dq}{Dt} &= \left(\frac{D\boldsymbol{\omega}}{Dt} - \boldsymbol{\omega} \cdot \nabla\mathbf{u} \right) \cdot \nabla\theta + \boldsymbol{\omega} \cdot \nabla \left(\frac{D\theta}{Dt} \right) \\ &= (Re^{-1}\Delta\boldsymbol{\omega} - \nabla^\perp\theta) \cdot \nabla\theta + \boldsymbol{\omega} \cdot \nabla((\sigma Re)^{-1}\Delta\theta) \\ &= \text{div}(Re^{-1}\Delta\mathbf{u} \times \nabla\theta + (\sigma Re)^{-1}\boldsymbol{\omega}\Delta\theta), \end{aligned} \quad (2.9)$$

where $\nabla^\perp\theta = \nabla\theta \times \hat{\mathbf{k}}$. The scalar product $\nabla^\perp\theta \cdot \nabla\theta = 0$ and the rest of the terms on the right-hand side of (2.9) have been regrouped as a divergence. On using $\text{div}\mathbf{u} = 0$ one may define \mathcal{U} through the equation

$$\partial_t q = -\text{div}(q\mathbf{u} - Re^{-1}\Delta\mathbf{u} \times \nabla\theta - (\sigma Re)^{-1}\boldsymbol{\omega}\Delta\theta) =: -\text{div}(q\mathcal{U}), \quad (2.10)$$

in which case $\text{div}\mathcal{U} \neq 0$, and

$$(\partial_t + \mathcal{U} \cdot \nabla)\theta = \partial_t\theta + \{\mathbf{u} - q^{-1}Re^{-1}[\Delta\mathbf{u} \times \nabla\theta + \sigma^{-1}\boldsymbol{\omega}\Delta\theta]\} \cdot \nabla\theta = 0. \quad (2.11)$$

The flux $\mathcal{J} = q\mathcal{U}$ was first introduced by Haynes and McIntyre in the context of their ‘impermeability theorem’ [11, 12]. There have been objections that \mathcal{U} is not a physical velocity [13, 14], which have been answered by McIntyre in [15] but in the context of this paper \mathcal{U} has been employed solely as a notational device. The remarkably simple form of (2.6) for the incompressible Euler case, in which $\mathcal{U} = \mathbf{u}$ and $\mathcal{D} = 0$, was derived first in [3–5]. Two versions of the proof of (2.6) are given in the appendix, the first using Lie derivatives and the second using conventional vector identities. \square

The right-hand side of (2.6) occurs because q is not a scalar function; rather it is a density (a volume form). However, because $\text{div}\mathbf{u} = 0$ for the incompressible Euler case, it follows that \mathcal{B} satisfies

$$\frac{D\mathcal{B}}{Dt} = \mathcal{B} \cdot \nabla\mathbf{u} \quad (2.12)$$

which is also the standard stretching equation for vorticity $\boldsymbol{\omega}$ on replacing \mathcal{B} with $\boldsymbol{\omega}$. The squared magnitude $|\mathcal{B}|^2$ satisfies

$$\frac{1}{2} \frac{D}{Dt} |\mathcal{B}|^2 = \mathcal{B} \cdot \mathbf{S}\mathcal{B} \approx \lambda^{(S)} |\mathcal{B}|^2, \quad (2.13)$$

where $\lambda^{(S)}(\mathbf{x}, t)$ is an estimate for an eigenvalue of the rate of strain matrix \mathbf{S} . Alignment of \mathcal{B} with a positive (negative) eigenvector of \mathbf{S} will produce exponential growth (decay), thus mimicking the stretching mechanism that produces the large vorticity intensities that develop locally in turbulence. Ohkitani [16] has studied Clebsch-decomposed solutions for $\boldsymbol{\omega} = \nabla f \times \nabla g$, where $Df/Dt = 0$ and $Dg/Dt = 0$.

Remark. Moffatt suggested the analogy between the magnetic field in a conducting fluid and the vorticity in an incompressible Euler flow [17] (see also [18]). Equation (2.12) continues this analogy. Moffatt’s detailed discussion of the topology of magnetic field lines is based on the concept of helicity that requires the existence of a vector potential \mathcal{A} that satisfies $\mathcal{B} = \text{curl } \mathcal{A}$, where

$$\mathcal{A} = \frac{1}{2}(Q\nabla\theta - \theta\nabla Q) + \nabla\psi. \tag{2.14}$$

The helicity H that results from this definition,

$$H = \int_V \mathcal{A} \cdot \mathcal{B} \, dV = \int_V \text{div}(\psi \mathcal{B}) \, dV = \oint_{\partial V} \psi \mathcal{B} \cdot \hat{n} \, dS, \tag{2.15}$$

measures the winding number, or knottedness of the lines of the divergence-free vector field \mathcal{B} . This helicity would vanish for homogeneous boundary conditions. However, if realistic topographies were taken into account, then the possibility for $H \neq 0$ would exist. The boundaries may therefore be an important generating source for helicity, thus allowing the formation of knots and linkages in the \mathcal{B} -field.

3. The case of the hydrostatic primitive equations

Many simulations of weather, climate and ocean circulation employ the hydrostatic version of the primitive equations (denoted as HPE). The major difference of HPE from the Navier–Stokes equations lies in the exclusion of the vertical velocity component $w(x, y, z, t)$ in the hydrostatic velocity field²

$$\mathbf{v}(x, y, z, t) = (u, v, 0). \tag{3.1}$$

However, this vertical component does appear in the transport velocity field $\mathbf{V} = (u, v, \varepsilon w)$, where ε is the Rossby number. The velocity field \mathbf{v} in (3.1) obeys the motion equation

$$\varepsilon(\partial_t + \mathbf{V} \cdot \nabla)\mathbf{v} + \hat{\mathbf{k}} \times \mathbf{v} + a_0 \hat{\mathbf{k}} \Theta = \varepsilon Re^{-1} \Delta \mathbf{v} - \nabla p, \tag{3.2}$$

and is solved in tandem with the incompressibility condition $\text{div } \mathbf{V} = \text{div } \mathbf{v} + \varepsilon w_z = 0$. The vertical velocity w has no evolution equation; it appears only in $\mathbf{V} \cdot \nabla$ and is determined from the vertical integral of the incompressibility condition $\text{div } \mathbf{V} = 0$. The z -derivative of the pressure field p and the dimensionless temperature Θ enter the problem through the hydrostatic equation

$$a_0 \Theta + p_z = 0, \tag{3.3}$$

which has been incorporated into (3.2) as its vertical component. The quantity a_0 is a constant, $\alpha_a = H/L \ll 1$ is the aspect ratio and R_a is the Rayleigh number, which comes from the non-dimensionalization of the original equations. By using the vector identity

$$\mathbf{V} \cdot \nabla \mathbf{v} = -\mathbf{V} \times \boldsymbol{\zeta} + \frac{1}{2} \nabla(u^2 + v^2) \tag{3.4}$$

in (3.2), the vorticity equation for

$$\boldsymbol{\zeta} = \text{curl } \mathbf{v} \tag{3.5}$$

is expressed as

$$(\partial_t + \mathbf{V} \cdot \nabla)\boldsymbol{\zeta} = (\sigma Re)^{-1} \Delta \boldsymbol{\zeta} + \boldsymbol{\zeta} \cdot \nabla \mathbf{V} + \text{curl } \mathbf{f}, \tag{3.6}$$

where $\mathbf{f} = -\varepsilon^{-1}(\hat{\mathbf{k}} \times \mathbf{v} + a_0 \hat{\mathbf{k}} \Theta)$. The dimensionless temperature Θ , with a specified heat transport term $h(x, y, z, t)$, satisfies

$$(\partial_t + \mathbf{V} \cdot \nabla)\Theta = (\sigma Re)^{-1} \Delta \Theta + h. \tag{3.7}$$

² The primitive equations as used for weather and climate prediction are defined on a corrected spherical grid.

Equations (3.6) and (3.7) for HPE correspond to those for the Navier–Stokes equations, with the additional h -term. Hence, the results in section 2 can be lifted over to HPE by defining

$$\mathbf{q} = \zeta \cdot \nabla \Theta \quad \text{and} \quad \mathbf{B} = \nabla Q \times \nabla \Theta, \quad (3.8)$$

where $Q(\mathbf{q})$ can be chosen as any smooth function of the potential vorticity \mathbf{q} , which itself obeys the relations

$$\partial_t \mathbf{q} + \text{div}(\mathbf{q}\mathbf{U}) = 0, \quad \mathbf{q}(\partial_t + \mathbf{U} \cdot \nabla)\Theta = 0. \quad (3.9)$$

Here, the formal transport velocity, \mathbf{U} , is defined from the vorticity flux density as

$$\mathbf{q}\mathbf{U} = \mathbf{q}\mathbf{V} - \{[Re^{-1}\Delta\mathbf{V} + \mathbf{f}] \times \nabla\Theta + [(\sigma Re)^{-1}\zeta\Delta\Theta + h]\}. \quad (3.10)$$

Clearly, \mathbf{U} includes the effects of rotation within \mathbf{f} and the heat transport term h : moreover, $\text{div}\mathbf{U} \neq 0$. As in the case of the Navier–Stokes equations this is not a physical velocity but is again a convenient mathematical device. Accordingly \mathbf{B} in (3.8) evolves according to the driven stretching relation

$$\partial_t \mathbf{B} - \text{curl}(\mathbf{U} \times \mathbf{B}) = \mathbf{D}, \quad (3.11)$$

where

$$\mathbf{D} = -\nabla(\mathbf{q}Q'(\mathbf{q})\text{div}\mathbf{U}) \times \nabla\Theta. \quad (3.12)$$

This equation is the analogue for HPE of equation (2.4) for the Navier–Stokes case. It implies that the time rate of change of the flux of \mathbf{B} in (3.8) through any surface \mathbf{S} that is transported at formal velocity \mathbf{U} is given by

$$\frac{d}{dt} \int_{\mathbf{S}(\mathbf{U})} \mathbf{B} \cdot d\mathbf{S} = \int_{\mathbf{S}(\mathbf{U})} \mathbf{D} \cdot d\mathbf{S}. \quad (3.13)$$

In particular, when the \mathbf{U} -transported surface is chosen to be a level set of temperature (whose normal vector is along $\nabla\Theta$) the right-hand side vanishes, as it should to maintain the tangency of \mathbf{B} to such surfaces. This means that the effects of PV gradient flux creation due to the right-hand side of (3.11) occur only on \mathbf{U} -transported surfaces that are *not* temperature iso-surfaces.

4. Conclusion

The equations for the evolution of the flux of PV gradient \mathcal{B} for Navier–Stokes in section 2 and \mathbf{B} for HPE in section 3 are the first two main results. Their left-hand sides represent the familiar flux transport form that governs the stretching processes while the second main feature is the derivation of the right-hand side \mathcal{D} and \mathbf{D} -terms; these divergence-less forcing terms deserve more investigation. Herring *et al* [19] have performed a computational study of vortex re-connection in the Navier–Stokes Boussinesq system (2.1) and (2.2). It is possible that the divergence-less vector \mathcal{D} may be the key to understanding this phenomenon with the left-hand side of (1.1) dominating for early to intermediate times until the effect of \mathcal{D} destroys the frozen-in property. A numerical study of the effect of \mathcal{D} may therefore be worthwhile.

In GFD, topography has been found to have some bearing on the nature of the topology of the \mathbf{B} -field, because helicity is generated at boundaries, and this potentially leads to the formation of knots and linkages in the \mathbf{B} -field lines. The atmospheric or oceanic events to which these knots and linkages would correspond are not wholly clear.

Investigation of steady-state balances of \mathbf{B} and its interaction with imposed steady coherent shear would also be interesting. In fact, analogous investigations of the spatial distribution of the PV flux are already underway in other contexts and, for example, have recently been studied via the data analysis of PV fronts at the sea surface (Czaja and Hausmann [20]). We

hope modern developments in observation and data analysis will soon provide new insight into the role and magnitude of the dynamical effects and balance effects caused by the transport of PV gradient flux along temperature iso-surfaces. In this regard, see, for instance, the recent paper by McWilliams *et al* [21] for a discussion of filamentary intensification in the ocean by processes similar to the stretching of \mathbf{B} . Likewise, in the atmosphere, the stretching of \mathbf{B} and the associated alignment properties of ∇q and $\nabla\theta$ are of interest, particularly in the region of the tropopause, as shown in figure 1.

Finally, the fundamental stretching mechanism in either HPE, or Navier–Stokes is the term $\mathbf{B} \cdot \nabla \mathbf{U}$. As already noted, the relation $\mathbf{B} \cdot (\mathbf{B} \cdot \nabla \mathbf{U}) = \mathbf{B} \cdot \mathbf{S} \mathbf{B}$ implies that alignment of \mathbf{B} along a positive eigenvector of the rate of strain matrix \mathbf{S} (noting that $\text{div } \mathbf{U} \neq 0$) will lead to exponential growth in \mathbf{B} . Thus, there will be a tendency for \mathbf{B} to stretch in these positive directions within a large coherent vortex. It has long been observed that large-scale vortices develop plateaus in PV and form steep cliff-like edges at the vortex boundary: see Rhines and Young [22] and Rhines [23]. As noted above, although the effect of the \mathcal{D} -term in (3.11) is not yet clear, it may play a significant role in the mechanism by which plateaus are formed in PV profiles, namely by the transport of PV gradient within a region of nonzero PV and along temperature iso-surfaces. The fact that PV gradient flux can be created along temperature iso-surfaces and can penetrate any other \mathbf{U} -transported surfaces may also help explain the ‘leakage’ or ‘erosion’ of PV gradient that is observed in certain regions of vortex boundaries.

Acknowledgments

We are grateful to P Berloff, M Bustamante, C J Cotter, R Hide, B Hoskins, N Klingaman, P Lynch and J T Stuart for discussions. DDH also thanks the Royal Society of London Wolfson Scheme for partial support.

Appendix. Derivation of equation (2.6)

Given the advective transport equations for temperature and potential vorticity,

$$\frac{D\theta}{Dt} = 0, \quad \frac{D}{Dt}(q \, d^3x) = (\partial_t q + \mathbf{u} \cdot \nabla q + q \, \text{div } \mathbf{u}) \, d^3x = 0, \quad (\text{A.1})$$

the evolution equation (2.6) for the quantity $\mathcal{B} = \nabla Q(q) \times \nabla\theta$ may be derived easily by using the notation of the exterior derivative (d) and the wedge product (\wedge):

$$\mathcal{B} \cdot d\mathbf{S} = (\nabla Q(q) \times \nabla\theta) \cdot d\mathbf{S} = dQ(q) \wedge d\theta. \quad (\text{A.2})$$

The advective time derivative of the leftmost term in this relation yields

$$\frac{D}{Dt}(\mathcal{B} \cdot d\mathbf{S}) = [\partial_t \mathcal{B} - \text{curl}(\mathbf{u} \times \mathcal{B})] \cdot d\mathbf{S} \quad \text{along} \quad \frac{D\mathbf{x}}{Dt} = \mathbf{u}. \quad (\text{A.3})$$

The advective time derivative of the rightmost term in (A.2) yields, using equations (A.1),

$$\begin{aligned} \frac{D}{Dt}(dQ(q) \wedge d\theta) &= d\left(\frac{DQ(q)}{Dt} \wedge d\theta\right) + dQ(q) \wedge d\left(\frac{D\theta}{Dt}\right) \\ &= -d(q Q' \, \text{div } \mathbf{u}) \wedge d\theta = \mathcal{D} \cdot d\mathbf{S}, \end{aligned} \quad (\text{A.4})$$

also along $D\mathbf{x}/Dt = \mathbf{u}$. For incompressible Euler flow, $\text{div } \mathbf{u} = 0$ and equation (2.6) arises by equating the rightmost terms in (A.3) and (A.4). When \mathbf{u} is replaced by \mathcal{U} for the Navier–Stokes equations, this yields a non-zero right-hand side because in this case $\text{div } \mathcal{U} \neq 0$.

The second version of the proof, with the notation $\omega_U = \text{curl} \mathbf{U}$, is simply a direct calculation:

$$\begin{aligned}
 \mathcal{B}_t &= (\nabla Q)_t \times (\nabla \theta) + (\nabla Q) \times (\nabla \theta)_t \\
 &= -\nabla[(q Q' \text{div} \mathbf{U}) + \mathbf{U} \cdot \nabla Q] \times (\nabla \theta) - (\nabla Q) \times [\nabla(\mathbf{U} \cdot \nabla \theta)] \\
 &= -\{\nabla(q Q' \text{div} \mathbf{U}) + \mathbf{U} \cdot \nabla(\nabla Q) + (\nabla Q) \cdot \nabla \mathbf{U} + (\nabla Q) \times \omega_U\} \times (\nabla \theta) \\
 &\quad - (\nabla Q) \times \{\mathbf{U} \cdot \nabla(\nabla \theta) + (\nabla \theta) \cdot \nabla \mathbf{U} + (\nabla \theta) \times \omega_U\} \\
 &= -\nabla(q Q' \text{div} \mathbf{U}) \times \nabla \theta - \mathbf{U} \cdot \nabla \mathcal{B} + (\nabla Q)(\omega_U \cdot \nabla \theta) - (\nabla \theta)(\omega_U \cdot \nabla Q) \\
 &\quad + (\nabla \theta) \times (\nabla Q \cdot \nabla \mathbf{U}) - (\nabla Q) \times (\nabla \theta \cdot \nabla \mathbf{U}) \\
 &= \text{curl}(\mathbf{u} \times \mathcal{B}) - \nabla(q Q' \text{div} \mathbf{U}) \times \nabla \theta.
 \end{aligned} \tag{A.5}$$

References

- [1] Hoskins B J 1982 *Annu. Rev. Fluid Mech.* **1** 131–51
- [2] Hoskins B J, McIntyre M E and Robertson A W 1985 *Q. J. R. Meteorol. Soc.* **111** 877–946
- [3] Kurgansky M V and Tatarskaya M S 1987 *Izv. Atmos. Ocean. Phys.* **23** 587–606
- [4] Kurgansky M V and Pisnichenko I A 2000 *J. Atmos. Sci.* **57** 822
- [5] Kurgansky M V 2002 *Adiabatic Invariants in Large-Scale Atmospheric Dynamics* (London: Taylor and Francis)
- [6] Schär C 1993 *J. Atmos. Sci.* **50** 1437–43
- [7] 2009 ECMWF Large-Scale Analyses: <http://www.met.rdg.ac.uk/Data/CurrentWeather>
- [8] Cao C and Titi E S 2007 *Ann. Math.* **166** 245–67
- [9] Ju N 2007 *Disc. Cont. Dyn. Syst.* **17** 159–79
- [10] Ertel H 1942 *Met. Z.* **59** 271–81
- [11] Haynes P and McIntyre M E 1987 *J. Atmos. Sci.* **44** 828–41
- [12] Haynes P and McIntyre M E 1990 *J. Atmos. Sci.* **47** 2021–31
- [13] Danielsen E F 1990 *J. Atmos. Sci.* **47** 2013–20
- [14] Viudez A 1999 *J. Atmos. Sci.* **56** 507–16
- [15] McIntyre M E 1990 Middle atmospheric dynamics and transport: some current challenges to our understanding *Dynamics, Transport and Photochemistry in the Middle Atmosphere of the Southern Hemisphere* ed A O'Neill (Amsterdam: Kluwer) pp 1–18
- [16] Ohkitani K 2008 *Physica D* **237** 2020–27
- [17] Moffatt H K 1978 *Magnetic Field Generation in Electrically Conducting Fluids* (Cambridge: Cambridge University Press)
- [18] Palmer T 1988 *Geo. Astro. Fluid Dyn.* **40** 133–45
- [19] Herring J K, Kerr R M and Rotunno R 1994 *J. Atmos. Sci.* **51** 35–47
- [20] Czaja A and Hausmann U 2009 Observations of entry and exit of potential vorticity at the sea surface *J. Phys. Oceanography* **39** 2280–94
- [21] McWilliams J C, Colas F and Molemaker M J 2009 *Geophys. Res. Lett.* **36** L18602
- [22] Rhines P B and Young W R 1982 *J. Fluid Mech.* **12** 347–67
- [23] Rhines P B 1993 *Oceanic General Circulation: Wave & Advection Dynamics. Modelling Oceanic Climate Interactions (NATO-ASI Series vol 1)* ed D Anderson and J Willebrandt (Dordrecht: Riedel) pp 67–149
- [24] Hoskins B J 2009 private communication